Fast Solver for Stokes Flow in 2D

Haiyang Wang, Leslie Greengard, Nils Jan Fredrik, Sam Potter

November 2, 2022

Abstract

In this paper, we exploited the *return to Poiseuille* phenomenon to build a solver for the interior plane Stokes flow with a domain that is union of *standard pieces*. Each standard piece's is a kind of pipe with inlets/outlets being long enough straight pipes. This enforces that the point of connection of two standard pieces is far away from any non-straight pipe. Then, *return to Poiseuille* hypothesis allow us to assume that each standard pieces have Poiseuille boundary conditions at inlets/outlets.

Once we pre-built the solvers for each standard pieces with Poiseuille boundary condition, we can then connect these standard pieces to form a arbitrarily large and complex pipe network. The solution of each standard pieces can be combined to get the solver of the global domain, based on the physics constraints of zero-net-flux and singular-valued-ness of pressure. Combining the local solvers would take at most $O(n^2)$ time, where n is the number of standard pieces. Much faster than solving the global problem directly.

1 Introduction

For plane Stokes flow, the biharmonic equation formulation are well known and developed within theory of complex variable from last century [9]. Various numerical schemes, such as boundary integral equation(BIE) and rational function approximation, have been developed accordingly [5, 12].

The *return to Poiseuille* phenomenon, or *Saint-Venant's principle* in the theory of plane elasticity, are well-established from the last century [3, 6, 8]. In particular, in a straight pipe with arbitrary incoming flow, the differences of Stokes flow and Poiseuille flow would decay exponentially fast toward the outlet. Quickly the flow would be indistinguishable from Poiseuille flow within machine-precision. Therefore it is a good numerical hypothesis to assume that the flow is Poiseuille at where the flow is far from non-straight parts of the pipe.

In this paper, we use the BIM from [5] to build solvers for multiple standard pieces with Poiseuille boundary condition in at inlets/outlets. The BIM is coupled with the biharmonic Fast Multiple Method (FMM) to reduce space and time complexity for the matrix-vector product [1]. Directly evaluating the BIM's solution near the boundary is known to be very inaccurate. Thus, we have adopted the methods from [13, 7] to correctly evaluate of layer potentials near the boundary. Finally, connection of standard pieces is by simply solving a linear equation, from the physics law of zero-net-flux and single-valued-ness of pressure. This linear equation depends merely on the flux and pressure at the point of connection of standard pipes, therefore can be solved instantly.

This paper is organized as follows. In Section 2, we define the Stokes boundary value problem, the corresponding biharmonic boundary value problem, and then the integral equation of it. We also mention the analytic evidence for the *return to Poiseuille* hypothesis. In Section 3, we presents the Nyestorm discretization of the integral equation. The numerical experiments of connecting standard pieces and numerical evidence for *return to Poiseuille* hypothesis are contained in Section 4, followed by conclusions in Section 5.

2 Mathematical Preliminaries

In this section, we first state the Stokes equation, translate it into the biharmonic equation, and then derive the Boundary Integral equation. This whole derivation is nothing new from [5]. Then, we will present the analytic bound for *return to Poiseuille* [6].

2.1 Stokes Boundary Value Problem

The plane linear Stokes equations are

$$\nu \Delta u = \frac{1}{\rho}\frac{\partial p}{\partial x}, \quad \nu \Delta v = \frac{1}{\rho}\frac{\partial p}{\partial y} \tag{1}$$

$$\frac{\partial u}{\partial x} + \frac{\partial v}{\partial y} = 0 \tag{2}$$

where u, v are components of velocity, ρ is the density, ν is the viscosity, and p is the pressure. Another important physics quantity, vorticity, is defined as $\zeta = u_y - v_x$.

We are interested in interior boundary value problem on a finite $(M+1)$-ply connected domain $D \subset \mathbb{R}^2$, with boundary $\partial D = \Gamma = \Gamma_0 \cup \Gamma_1 \cup \cdots \cup \Gamma_M$, where Γ_0 is the exterior boundary, and $\Gamma_1, \cdots, \Gamma_M$ are the interior boundaries. We restrict our attention to problems where the velocity is given on the boundary:

$$u = h_2(t), \quad v = -h_1(t), \quad t \in \Gamma \tag{3}$$

2.2 The Biharmonic Potential

Biharmonic Stream Function. (2) implies the existence of the stream function $W(x, y)$ such that:

$$\frac{\partial W}{\partial x} = -v, \quad \frac{\partial W}{\partial y} = u \tag{4}$$

Following (1,2), it is easy to see that the stream function satisfies the biharmonic equation (5), and the boundary velocity conditions (3) can be understood as the boundary conditions

for the biharmonic equation (6):

$$\Delta^2 W(x,y) = \Delta\zeta = 0, \qquad (x,y) \in D \tag{5}$$

$$\frac{\partial W}{\partial x} = h_1(t), \quad \frac{\partial W}{\partial y} = h_2(t), \qquad t \in \Gamma \tag{6}$$

Goursat's Formula. It's been long established that any plane biharmonic function $W(x,y)$ can be expressed by Goursat's formula

$$W(x,y) = \mathrm{Re}(\bar{z}\phi(z) + \chi(z)) \tag{7}$$

where ϕ, χ are analytic functions of complex variable $z = x+yi$. In the following, we will be identifying $(x,y) \in \mathbb{R}^2$ with $x+yi \in \mathbb{C}$ as a convenient abuse of notation.

The Muskhelishvili's formula connects velocity of Stokes flow with the Goursat's formula:

$$u(x,y) + iv(x,y) = \phi(z) + z\overline{\phi'(z)} + \overline{\psi(z)} \tag{8}$$

where $\psi = \chi'$. This transforms the biharmonic boundary condition (6) into

$$\phi(t) + t\overline{\phi'(t)} + \overline{\psi(t)} = h(t), \quad t \in \Gamma \tag{9}$$

where $h(t) = h_1(t) + ih_2(t)$, and t is understood as a complex variable.

For Stokes flow, there is another formula connecting pressure and vorticity with the Goursat's functions

$$\zeta + \frac{i}{\nu}p = 4\phi'(z) \tag{10}$$

Sherman-Lauricella Representation. The boundary integral equation is an ansatz based on of an extension of Sherman-Lauricella representation proposed in [5].

$$\phi(z) = \frac{1}{2\pi i}\int_\Gamma \frac{\omega(\xi)}{\xi - z}d\xi + \sum_{k=1}^{M} C_k \log(z - z_k) \tag{11}$$

$$\psi(z) = \frac{1}{2\pi i}\int_\Gamma \frac{\overline{\omega(\xi)}d\xi + \omega(\xi)\overline{d\xi}}{\xi - z} - \frac{1}{2\pi i}\int_\Gamma \frac{\bar{\xi}\omega(\xi)}{(\xi - z)^2}d\xi + \sum_{k=1}^{M}\left(\frac{b_k}{z - z_k} + \overline{C}_k \log(z - z_k) - C_k\frac{\overline{z}_k}{z - z_k}\right) \tag{12}$$

where ω is an unknown complex density on Γ to be solved for, z_k are arbitrarily prescribed point inside the component curves Γ_k, and C_k, b_k are constants defined by

$$C_k = \int_{\Gamma_k}\omega(\xi)|d\xi|, \quad b_k = 2\,\mathrm{Im}\int_{\Gamma_k}\overline{\omega(\xi)}d\xi \tag{13}$$

Boundary Integral Equation. Letting a point z in the interior of D approach to a point on the boundary $t \in \Gamma$, the classical formulae for the limiting values of Cauchy-type integral gives us the an integral equation for ω:

$$\omega(t) + \frac{1}{\pi}\int_\Gamma \omega(\xi)d\ln\frac{\xi - t}{\overline{\xi - t}} - \frac{1}{2\pi i}\int_\Gamma \overline{\omega(\xi)}d\frac{\xi - t}{\overline{\xi - t}} + \sum_{k=1}^{M}\left(\frac{\bar{b}_k}{\overline{t - z_k}} + 2C_k\log|t - z_k| + \bar{C}_k\frac{t - z_k}{\overline{t - z_k}}\right) + \frac{\bar{b}_0}{\bar{t} - \bar{z}^*} = h(t) \tag{14}$$

the extra term $\frac{\bar{b}_0}{\bar{t} - \bar{z}^*}$ vanishes when the zero-net-flux condition $\mathrm{Re}\int_\Gamma \bar{h}(t)dt = 0$ is satisfied. The invertibility of this integral equation is similar to the standard proof of invertibility for elasticity problems [10], hence omitted.

2.3 Return to Poiseuille

On the domain of a semi-infinite pipe $D_L = \{(x,y) \mid x \geq 0, |y| \leq L\}$, with the boundaries

$$\begin{aligned}\Gamma_L &= \Gamma_L^1 \cup\Gamma_L^2 \cup\Gamma_L^3 \\ &= \{(0,y)||y| \leq L\} \cup\{(x,L)|x \geq 0\} \cup\{(x,-L) \mid x \geq 0\}\end{aligned} \tag{15}$$

where Γ_L^2, Γ_L^3 are walls with the non-slippery boundary conditions, and Γ_L^1 is the only part with non-zero boundary conditions. Return to Poiseuille means that regardless of the boundary conditions on Γ_L^1, the flow's profile at $x = l$ will converge Poiseuille flow as l approaches to infinity. Without lost of generality, assuming there is zero net flux across Γ_L^1, return to Poiseuille is equivalent to return to zero flow.

The biharmonic BVP can then written as

$$\frac{\partial W}{\partial y} = W(x,y) = 0, \quad (x,y) \in \Gamma_L^2 \cup \Gamma_L^3 \tag{16}$$

$$\frac{\partial W}{\partial x} = f(y), \quad \frac{\partial W}{\partial y} = g(y), \quad |y| \leq L \tag{17}$$

where are f, g are some functions with $f(\pm L) = g(\pm L) = \int_{-L}^{L} g(y)dy = 0$.

This biharmonic BVP is identical to the "self-equilibrated" traction BVP in the theory of elasticity studied in [6, 8, 3]. When f''', g''' are of bounded variation, this problem has a unique solution spanned by the Papkovich-Fadle eigenfunctions [6]. The first eigenfunction is dominated by $e^{-xk/2L}$, where

$$k \simeq 4.2$$

is the smallest positive real parts of the roots of the transcendental equation $\sin^2\lambda - \lambda^2 = 0$. This gives the decay rate of return to Poiseuille hypothesis, whice agrees with [numerical experiment to be included later].

3 Description of Numerical Methods

In this section, we will first present Nyström discretization of boundary integral equation (14), and then we briefly explain the discretization of the boundary.

3.1 Boundary Integral equation

The boundary curve Γ_k is discretized into N_k points $t_i^k = t^k(a_i^k) \in \Gamma_k$, for a given parametrization $t^k : [A_k, A_{k+1}] \to \Gamma_k$ and $a_i^k \in [A_k, A_{k+1}]$ are the parameter. Associate to each point t_j^k are the unknown complex density ω_j^k, the derivative $d_j^k = t^{k\prime}(a_j^k)$, and the quadrature weight w_j^k. In total, we have $N = \sum_{k=0}^{M} N_k$ points. Nyström discretization of (14) is

$$\omega_j^k + \sum_{m=0}^{M}\sum_{n=1}^{N_k} K_1(t_j^k, t_n^m)\omega_j^k + \sum_{m=0}^{M}\sum_{n=1}^{N_k} K_2(t_j^k, t_n^m)\overline{\omega_j^k} = h_j^k \tag{18}$$

where $h_j^k = h(t_j^k)$ and the kernels K_1, K_2 are given by

$$K_1(t_j^k, t_n^m) = \frac{1}{\pi}\,\mathrm{Im}\left(\frac{d_n^m}{t_n^m - t_j^k}\right) w_n^m + \delta_m \left(\frac{i w_n^m \overline{d_n^m}}{\overline{t_j^k - z_m}} + 2 w_n^m \log|t_j^k - z_m| \right) \tag{19}$$

$$K_2(t_j^k, t_n^m) = \frac{1}{\pi} \frac{\mathrm{Im}((t_n^m - t_j^k)\overline{d_n^m})}{(\overline{t_n^m - t_j^k})^2} w_n^m + \delta_m \left(-\frac{i w_n^m d_n^m}{\overline{t_j^k - z_m}} + \frac{w_n^m (t_j^k - z_m)}{\overline{t_j^k - z_m}} \right) \tag{20}$$

where $\delta_m = 1$ excepts for $\delta_0 = 0$. And in the limiting case of $t_j^k = t_n^m$, the corresponding value can be seen as the limiting value:

$$K_1(t_j^k, t_j^k) = \frac{w_j^k \kappa_j^k |d_j^k|}{2\pi} + \delta_k(\cdots) \tag{21}$$

$$K_2(t_j^k, t_j^k) = -\frac{w_j^k \kappa_j^k (d_j^k)^2}{2\pi |d_j^k|} + \delta_k(\cdots) \tag{22}$$

where κ_j^k is the signed quadrature at the point t_j^k.

The RHS of (18) for any density ω is evaluated by biharmonic fmm [1]. And this Nyström discretization is regarded as an matrix equation, by separating the real part and imaginary part, and then solved iteratively using generalized minimum residual method GMRES [11].

Evaluation of the layer potentials near boundary is done as in [13].

3.2 Geometry of the Boundary

The key to spectral convergence of GMRES is to have smooth boundary, or for piecewise smooth boundary, one can use special treatment as in [13] to ensure the spectral convergence is preserved. Here for this paper, we uses tricks to ensure the geometry is smooth. We adopted the ideas from [4, 2] to smooth the corners of the boundary by convolution, and added superficial caps at the inflows and outflows. [insert a figure here].

The return to Poiseuille hypothesis means that putting the Poiseuille boundary condition on the superficial cap, is effectively the same as putting the Poiseuille boundary condition on the rectangular inlet/outlet.

And each boundary component is adaptively discretized into Gauss-Legendre panels, as described in [13].

4 Numerical Results and Discussion

4.1 numerical evidence of return to poiseuille

The numerical evidence for return to Poiseuille phenomenon is demonstrated on a straight pipe of width 1 and length 8. On the left boundary, a random velocity profile is imposed, and zero velocity condition is imposed on the rest of the curve.

Figure 1a shows that the rate of returning to the zero flow is agreed with the predicted rate from Section 2.3 until the 14th digits of accuracy. Figure 1b is a color plot where the color indicates the $\log_{10}$ of absolute value of the velocity, pressure, and vorticity. We can clearly observe presence of the eigenfunction from each of the three color plots. Except for near the right end of the pipe, where bizarre patterns started to appear near the boundaries. The author believes that this is due to the numerical error from the near panel evaluation scheme from [13], and this is the reason why Return to Poiseuille phenomenon stops demonstrating as predicted at 14th digits of accuracy. It is worth-noting that the near panel evaluation scheme is only applied in the post-processing, which does not involve in the GMRES iterations. Therefore, despite that the we can only have 14th digits of accuracy for velocity, pressure, and vorticity, the complex density ω does not suffer from this numerical limitation.

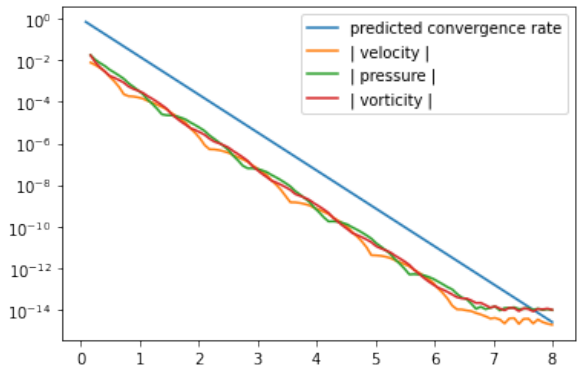

(a) Convergence plot for return to zero flow.

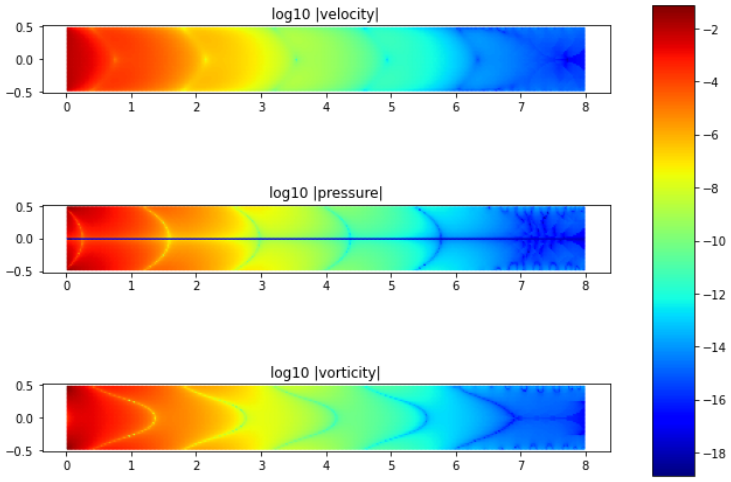

(b) Color plot of the velocity, vorticity, and pressure

Figure 1: Return to Poiseuille flow in a straight pipe.

4.2 a complicated network of pipes to show the power of this method

5 Conclusions

5.1 summarize what I've done

5.2 outlook. What other work might be followed?

References

[1] Flatironinstitute/fmm2d.

[2] Joar Bagge and Anna-Karin Tornberg. Highly accurate special quadrature methods for Stokesian particle suspensions in confined geometries. 93(7):2175–2224.

[3] Horgan Co. Recent developments concerning Saint-Venant's principle,". In *In Advances in Applied Mechanics, TY Wu and JW Hutchinson (Eds), Vol 23,*, pages 179–269. Academic Press,.

[4] Charles L. Epstein and Michael O'Neil. Smoothed corners and scattered waves.

[5] Leslie Greengard, Mary Catherine Kropinski, and Anita Mayo. Integral Equation Methods for Stokes Flow and Isotropic Elasticity in the Plane. 125(2):403–414.

[6] R. D. Gregory. The traction boundary value problem for the elastostatic semi-infinite strip; existence of solution, and completeness of the Papkovich-Fadle eigenfunctions. 10(3):295–327.

[7] Johan Helsing and Rikard Ojala. On the evaluation of layer potentials close to their sources. 227(5):2899–2921.

[8] C. O. HORGAN. DECAY ESTIMATES FOR THE BIHARMONIC EQUATION WITH APPLICATIONS TO SAINT-VENANT PRINCIPLES IN PLANE ELASTICITY AND STOKES FLOWS. 47(1):147–157.

[9] O. A. Ladyzhenskaya, Richard A. Silverman, Jacob T. Schwartz, and Jacques E. Romain. *The Mathematical Theory of Viscous Incompressible Flow*. 17(2):57–58.

[10] N. I. Muskhelishvili. *Some Basic Problems of the Mathematical Theory of Elasticity*. Springer Netherlands.

[11] Youcef Saad and Martin H. Schultz. GMRES: A Generalized Minimal Residual Algorithm for Solving Nonsymmetric Linear Systems. 7(3):856–869.

[12] Lloyd N. Trefethen. *Approximation Theory and Approximation Practice, Extended Edition*. Society for Industrial and Applied Mathematics.

[13] Bowei Wu, Hai Zhu, Alex Barnett, and Shravan Veerapaneni. Solution of Stokes flow in complex nonsmooth 2D geometries via a linear-scaling high-order adaptive integral equation scheme. 410:109361.